Structural, functional, and tissue distribution analysis of human transferrin receptor-2 by murine monoclonal antibodies and a polyclonal antiserum

Silvia Deaglio, Andrea Capobianco, Angelita Calì, Francesca Bellora, Federica Alberti, Luisella Righi, Anna Sapino, Clara Camaschella, and Fabio Malavasi

Human transferrin receptor-2 (TFR-2) is a protein highly homologous to TFR-1/CD71 and is endowed with the ability to bind transferrin (TF) with low affinity. High levels of TFR-2 mRNA were found in the liver and in erythroid precursors. Mutations affecting the *TFR-2* gene led to hemochromatosis type 3, a form of inherited iron overload. Several issues on distribution and function of the receptor were answered by raising a panel of 9 monoclonal antibodies specific for TFR-2 by immunizing mice with murine fibroblasts transfected with the human TFR-2 cDNA. A polyclonal antiserum was also produced in mice immunized with 3 peptides derived from the TFR-2 sequence, exploiting an innovative technique. The specificity of all the reagents produced was confirmed by reactivity with TFR-2$^+$ target cells and simultaneous negativity with TFR-1$^+$ cells. Western blot analyses showed a dominant chain of approximately 90 kDa in TFR-2 transfectants and HepG2 cell line. Analysis of distribution in normal tissues and in representative cell lines revealed that TFR-2 displays a restricted expression pattern—it is present at high levels in hepatocytes and in the epithelial cells of the small intestine, including the duodenal crypts. Exposure of human TFR-2$^+$ cells to TF-bound iron is followed by a significant up-regulation and relocalization of membrane TFR-2. The tissue distribution pattern, the behavior following exposure to iron-loaded TF, and the features of the disease resulting from TFR-2 inactivation support the hypothesis that TFR-2 contributes to body iron sensing. (Blood. 2002;100:3782-3789)

Introduction

Iron participates in a wide variety of key metabolic processes of living organisms, including oxygen and electron transport and DNA synthesis. Transferrin receptor-1 (TFR-1), a homodimeric membrane glycoprotein clustered as CD71, plays a major role in the uptake of transferrin-bound iron.[1,2] Besides dominant TFR-1–mediated endocytosis, cellular iron uptake may be obtained through TFR-1–independent pathways.[3] Human TFR-2 is a newly identified member of the TFR family, serendipitously cloned during an attempt to isolate genes encoding transcription factors.[4] Based on the predicted amino acid sequence, TFR-2 is a type 2 transmembrane protein with 66% similarity to TFR-1 in the extracellular domain.[4]

Major differences between TFR-2 and TFR-1 concern mRNA tissue distribution and regulation of expression. Northern blot analysis and reverse transcription–polymerase chain reaction (RT-PCR) showed that the message for TFR-2 is predominantly detected in the liver and, among a panel of cell lines, in HepG2 (hepatocarcinoma) and K562 (erythroleukemia).[4] In addition, high levels of TFR-2 mRNA are found in normal early erythroid precursors and in myeloid leukemic blasts.[5]

TFR-2 is hypothesized to bind iron-loaded transferrin (TF) and to transport iron into the cytosol, as inferred from a model of Chinese hamster ovary cells transfected with TFR-2 and constitutively lacking TFR-1.[4,6] However, the function of TFR-2 is not equivalent to that of TFR-1: murine TFR-2 does not replace TFR-1 functions, and TFR-1–deficient mice do not survive beyond embryonic day 12.5 because of neurologic abnormalities and severe anemia.[7] Moreover, mice with only one functional TFR-1 allele have mild tissue iron depletion,[7] whereas the inactivation of TFR-2 in humans results in hemochromatosis (HH) type 3, a genetic form of iron overload.[8-10]

Regulation of TFR-2 expression is clearly distinct from that of TFR-1. The most striking differences are the lack of iron-responsive elements in the TFR-2 mRNA and the absence of the iron-dependent posttranscriptional regulation that characterizes other key genes of iron metabolism.[6] At variance with TFR-1, TFR-2 is apparently insensitive to tissue iron status, and it is not down-modulated in a murine model of HH.[11,12]

This work reports on the production of a panel of monoclonal antibodies (mAbs) and a murine polyclonal antiserum specific for TFR-2. These reagents were used to analyze the tissue distribution of TFR-2 and to study its behavior following exposure to the physiologic ligand.

From the Laboratory of Immunogenetics, Department of Genetics, Biology, and Biochemistry, the Experimental Medicine Research Center, the Department of Clinical and Biological Sciences, and the Department of Biomedical Sciences and Human Oncology, University of Turin Medical School, Italy.

Submitted January 10, 2002; accepted June 18, 2002. Prepublished online as *Blood* First Edition Paper, July 5, 2002; DOI 10.1182/blood-2002-01-0076.

Supported by grants from AIRC, Special Projects AIDS (Istituto Superiore di Sanità), Biotechnology (CNR/MURST), and Cofinanziamento (MURST 40%) (F.M.), from Telethon grant GP00255Y01, E.U. contract QLK6-1999-02237, and MURST 40% (C.C.). The Compagnia di SanPaolo and the Fondazione Internazionale di Ricerche in Medicina Sperimentale provided valuable financial contributions. S.D. is a student of the Postgraduate School of Medical Oncology. L.R. is a PhD fellow in Human Oncology, University of Turin Medical School, Italy.

Reprints: Fabio Malavasi, Laboratory of Immunogenetics, Department of Genetics, Biology, and Biochemistry, University of Turin Medical School, via Santena, 19, 10126 Turin, Italy; e-mail: fabio.malavasi@unito.it.

The publication costs of this article were defrayed in part by page charge payment. Therefore, and solely to indicate this fact, this article is hereby marked "advertisement" in accordance with 18 U.S.C. section 1734.

Materials and methods

Preparation of a construct enclosing the full-length cDNA of human TFR-2

TFR-2 cDNA was prepared by RT-PCR starting from the poly-A RNA of the HepG2 cell line. Touchdown PCR was carried out using Expand long-template PCR system (Boehringer-Mannheim, Mannheim, Germany). After reverse transcription (42°C, 60 minutes, terminated by heating for 2 minutes at 94°C), PCR was performed for 8 cycles (denaturation: 1 minute, 94°C; annealing: 1 minute, 64°C, with a lowering increment of 2°C/cycle; elongation: 5 minutes, 68°C). Thermocycling was continued for up to 38 cycles (denaturation: 1 minute, 94°C; annealing: 1 minute, 56°C; elongation: 7 minutes, 68°C). All RT-PCR reactions were performed using an automated thermal cycler (Perkin Elmer, Boston, MA) with primers selected according to the published sequence.

An aliquot (1 μL) of the reaction product was ligated to a pcDNA3.1 expression vector by the TA-Cloning system, and transformation was carried out on *Escherichia coli* TOP10 cells (all from Invitrogen, Carlsbad, CA). Positive transformants were analyzed for the presence and correct orientation of TFR-2 cDNA by PCR and by digestion with the *Nco*I restriction enzyme (New England Biolabs, Beverly, MA) and partial sequencing. Results confirmed that TFR-2 was identical to the reported one (GenBank accession number, XM 005011). Selected transformants, indicated as TFR-2/pcDNA3.1, were grown in LB medium and purified by the Quantum Prep plasmid midiprep kit (Bio-Rad, Hercules, CA).

Transfection and selection

Twenty micrograms TFR-2/pcDNA3.1 was linearized by treatment with 20 IU/mg *Sca*I restriction enzyme (New England Biolabs) and was used to stably transfect NIH-3T3 cells by electroporation (250 V/0.4 cm and 960 μF). After 2-week incubation in a medium containing 1 mg/mL G418 (Sigma-Aldrich, Milan, Italy), neomycin-resistant colonies were isolated, and the presence of the TFR-2 cDNA was checked by RT-PCR. As a final confirmation of the identity of the cDNA, a restriction enzyme map and internal-fragment PCR amplification were obtained. A fragment corresponding to exons 3 to 4 of TFR-2 was amplified using the primer forward 5′-GGGCCTTCCTACTGGG-3′, reverse 5′-CCACACGTGGTCCAGGTTCTGGGGGGA-3′.[4] Positive colonies were isolated and recloned by serial dilution to ensure clonality. NIH-3T3 cells were similarly transfected with an empty pcDNA3.1 vector and were selected using G418.[13]

Cells and specimens

HepG2 and K562 cell lines were selected in view of their high levels of TFR-2 RNA expression. Murine L-fibroblasts transfected with the human TFR-1 (L-CD71$^+$) were obtained as described.[14] Solid tumor and hematologic cell lines used in the study are listed in Table 1.

The study included specimens derived from human organs obtained from the Pathology Department of the University of Turin. Biopsy samples of normal tissues were obtained following ablative surgery for various malignancies from patients who did not undergo chemotherapy or radiotherapy.

Peptides and reagents

Three peptides (SQDPPKPSLSSQ, amino acids 305-316; RARGVDPVGR, amino acids 260-269; NSSGTPGATSSTGF, amino acids 754-767) were selected from the published TFR-2 sequence, synthesized, and purchased from Primm (Milan, Italy). Peptides were selected as encoding the most representative regions of the human TFR-2 molecule—that is, those marking sequences not shared with TFR-1 and different from the murine sequences.

Iron-poor (APO) and iron-saturated (HOLO) TF were purchased from Sigma. Anti-CD71 mAbs used included CB26 and MyBe, locally produced and purified,[14] and H68.4, purchased from Zymed (San Francisco, CA). Anti-HLA class 1 mAb NL02[15] was used as control.

Table 1. Expression of TFR-2 in a variety of cells

Name	Origin	MFI G/14C2	MFI G/1C11	MFI Control
HepG2	Hepatoma	73	69	4
CFPAC-1	Pancreatic carcinoma	13	15	5
SW480	Colon carcinoma	4	18	4
KATO III	Stomach carcinoma	48	20	3
T47D	Breast carcinoma	11	15	3
DU145	Prostate carcinoma	67	81	7
LAN-1	Neuroblastoma	58	65	5
U251	Glioma	26	10	2
K562	CML	346	69	5
NB-4	AML	7	6	6
HL-60	AML	3	5	2
U937	AML	3	3	3
Jurkat	T-ALL	6	4	4
YT	NK-ALL	5	2	3
NKL	NK-ALL	5	6	4
Raji	B lymphoma	14	18	8
SKMM-1	Myeloma	39	15	3
RPMI 8226	Myeloma	17	9	7
FF	Amnion	3	2	2
HUVEC	Endothelium	4	4	4

FF indicates fetal fibroblast; HUVEC, human umbilical cord endothelial cell; CML, chronic myeloid leukemia; AML, acute myeloid leukemia; and ALL, acute lymphoblastic leukemia.

Antibody production

A panel of specific murine mAbs was produced using NIH-3T3/TFR-2/4B1 as an immunizer. Briefly, 2×10^5 transfectants were resuspended in 200 μL phosphate-buffered saline and were injected into the spleens of anesthetized female Balb/c mice (22-25 g) through a direct opening of the peritoneum under surgical conditions.[16] The same set of mice underwent chronic boosting using 2×10^5 cells injected intravenously at approximately 20-day intervals for 3 months. Four days after the last injection, the spleen was removed for fusion with the P3.X63-Ag8.653 cell line using PEG 1500-1700 (Sigma).[17]

Spent media of the primary cultures were screened on NIH-3T3/TFR-2/4B1 cells and simultaneously on control wild-type NIH-3T3 cells by means of indirect immunofluorescence (IIF) and visual observation to select the binding mAbs. Positive clones were further tested to confirm the reactivities with HepG2 and K562 cell lines, reported as expressing TFR-2 mRNA.[4]

Primary cultures fulfilling the binding requisites of the selection grid were cloned 3 times by limiting dilution and subsequently were grown as tumor ascites in pristane-primed mice. The mAbs were purified using a high-performance liquid chromatography technique after purification on protein A.[18]

A polyclonal antiserum was obtained in Balb/c mice immunized with a mixture of 3 different peptides (see above). The mice were injected intrasplenically with approximately 20 μg of each peptide and received successive intraperitoneal boosts with equal amounts of peptides and appropriate amounts of Freund incomplete adjuvant. Once the titer of circulating antibodies reached detectable levels in an enzyme immunoassay system, the volume of the biologic fluids of the mice was artificially expanded by inducing the growth of an intraperitoneal tumor ascites, secondary to the injection of pristane-primed mice with P3.X63-Ag8.653 cells, a murine nonproducing and nonsecreting myeloma.

Western blot analysis of the target structure

NIH-3T3/TFR-2/4B1, mock-transfected NIH-3T3, HepG2, K562, HL-60, and L-CD71$^+$ cells were lysed in 1% NP-40 lysis buffer (20 mM HEPES [N-2-hydroxyethylpiperazine-N'-2-ethanesulfonic acid], pH 7.6, 150 mM NaCl, 50 mM NaF, 1 mM Na_3VO_4, 1 mM EGTA [ethyleneglycoltetraacetic acid], 50 μM phenilarsine oxide, 10 μM iodoacetamide and antipain, chymostatin, leupeptin, and pepstatin) for 20 minutes on ice. After the removal of nuclei by centrifugation, an aliquot of the lysates was run in 6% sodium dodecyl sulfate–polyacrylamide gel electrophoresis (SDS-PAGE)

under reducing conditions and was transblotted onto nitrocellulose membranes (Amersham, Little Chalfont, Buckinghamshire, United Kingdom), as described.[19] Immunoblotting was performed using as probe either the mAbs or the polyclonal antiserum, later highlighted by means of rabbit immunoglobulin conjugated to horseradish peroxidase (Sigma). The reaction was revealed using a CDP-STAR chemiluminescence reagent (NEN-Life Science Products, Boston, MA), and the membranes were subjected to autoradiography.

Indirect immunofluorescence

Surface expression of TFR-2 was determined by IIF and flow cytometric analysis (FACSort; Becton Dickinson, Milan, Italy). Target cells (2×10^5) were incubated with 1 μg indicated mAb; the secondary reagent was a fluorescein isothiocyanate (FITC)–conjugated $F(ab')_2$ fragment of a goat anti–mouse immunoglobulin antibody (Caltag, Burlingame, CA). Intensity of fluorescence was recorded on a logarithmic scale by scoring at least 10 000 cells/sample; background fluorescence intensity was obtained by incubating the cells with the goat anti–mouse immunoglobulin reagent alone.

Tissue distribution

Distribution of TFR-2, as recognized by the different mAbs, was examined on tissues using formalin-fixed, paraffin-embedded tissues of surgical specimens. Endogenous peroxidase and endogenous biotin were inhibited as described elsewhere.[20] Heat-induced antigen retrieval was performed by pretreatment in a microwave oven (3 times for 3 minutes at 750 W) of the sections incubated in 1 mM EDTA (ethylenediaminetetraacetic acid) buffer (pH 8.0) or in 10 mM citrate buffer (pH 6.0).[21] After incubation with the specific mAb, the reaction was revealed using the universal LSAB 2 streptavidin kit (DAKO, Glostrup, Denmark).

Analysis of TF–TFR-2 interactions

Adherent cell lines HepG2 and U251 were grown on glass coverslips and treated at 37°C with APO-TF and HOLO-TF, used at concentrations varying from 10 to 50 μg/mL. The experiment was stopped at 30-minute intervals, with a maximum lapse of 8 hours. Cells were then fixed and permeabilized (ice-cold methanol [5 minutes at −20°C], followed by ice-cold acetone [5 seconds at −20°C]) and were incubated (1 hour at 37°C) with the mAb under analysis. After extensive washing, an FITC-conjugated $F(ab')_2$ fragment of a goat anti–mouse immunoglobulin antibody was added (30 minutes at 37°C). Coverslips were mounted on slides using a water-soluble mountant and were analyzed with a C-VIEW–12-BUND camera fitted to an Olympus 1 × 70 microscope (Olympus, Milan, Italy), with the images collected using the ANALYSIS software (OLYMPUS, Milan, Italy). K562 cells were stained in suspension for TFR-2 and TFR-1 expressions after identical treatments and were evaluated by cytofluorography using FACSort equipment, as described above.

Results

Generation of murine fibroblasts stably expressing the human TFR-2 transcript

Murine NIH-3T3 fibroblastoid cells, electroporated in the presence of a pcDNA3.1 vector enclosing the full-length human TFR-2 construct and selected for growing in G418-conditioned medium, were used as immunizers and as target cells for the successive experiments. Cells surviving G418 were further selected on the basis of the RT-PCR results for TFR-2 presence. Clone 4B1 fulfilled all the requisites and was subcloned by limiting dilution, constantly kept under metabolic selection, and referred to as NIH-3T3/TFR-2/4B1. Transfection with the empty plasmid resulted in the production of G418-resistant clones not expressing TFR-2 and hereinafter referred to as mock-transfected NIH-3T3.

Production of monoclonal and polyclonal antibodies

NIH-3T3/TFR-2/4B1 cells were used to immunize Balb/c mice directly into the spleen. IIF analysis of spent media of the primary cultures using NIH-3T3/TFR-2/4B1 and, simultaneously, control mock-transfected NIH-3T3 cells as targets allowed the selection of a panel of 9 mAbs potentially specific for TFR-2 (Figure 1). The reactivity pattern was confirmed by using human cell lines previously reported as containing high amounts of mRNA for TFR-2, namely HepG2 and K562. All mAbs clearly reacted with HepG2 cells, with similar staining profiles in terms of percentage of reactive cells and fluorescence intensity (Figure 2). Reactivity with K562 split the selected panel in mAb binding to more than 60% of the cells—G/5F8 (immunoglobulin M [IgM]), G/14C2 (IgG2b), G/8E7 (IgG2b), G/14E8 (IgG2b), and G/7F5 (IgG1) mAbs, referred to as group A—and a group binding to less than 30% of the cells—G/5B5, G/5C5, G/5B3, and G/1C11 mAbs, referred to as group B—and all of IgM isotype. This panel of mAbs was then used for detailed structural and functional analysis of the TFR-2 receptor.

A murine polyclonal antiserum was simultaneously raised in Balb/c mice to avoid the limits of comparison among antibodies raised in different animals against the same target. Mice were immunized with a mixture of 3 peptides, selected as encoding representative regions of the TFR-2 molecule. The original method adopted for expanding in vivo the mass of the body fluids of the donor mice was fruitful, and 2 animals yielded a volume of polyclonal ascites approximately similar to that obtained from the

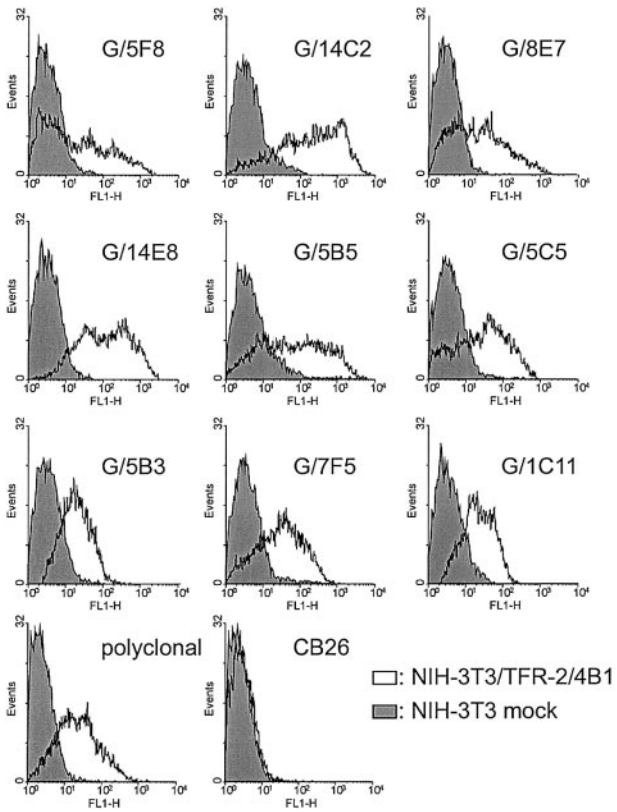

Figure 1. Reactivity of the mAbs and polyclonal antiserum against NIH-3T3/TFR-2/4B1 and control mock-transfected NIH-3T3 cells. Primary fusion cultures were screened for binding to murine fibroblasts transfected with the human *TFR-2* gene (NIH-3T3/TFR-2/4B1, white histograms), using mock-transfected NIH-3T3 cells (gray profiles) as negative control. The selection grid allowed the identification of 9 specific mAbs. A polyclonal antiserum, obtained by immunizing Balb/c mice with a mixture of 3 peptides derived from the TFR-2 sequence, displayed the same reactivity. CB26, a TFR-1–specific mAb, did not cross-react with NIH-3T3/TFR-2/4B1 cells. X-axis, fluorescence intensity/cells; y-axis, number of cells registered/channel.

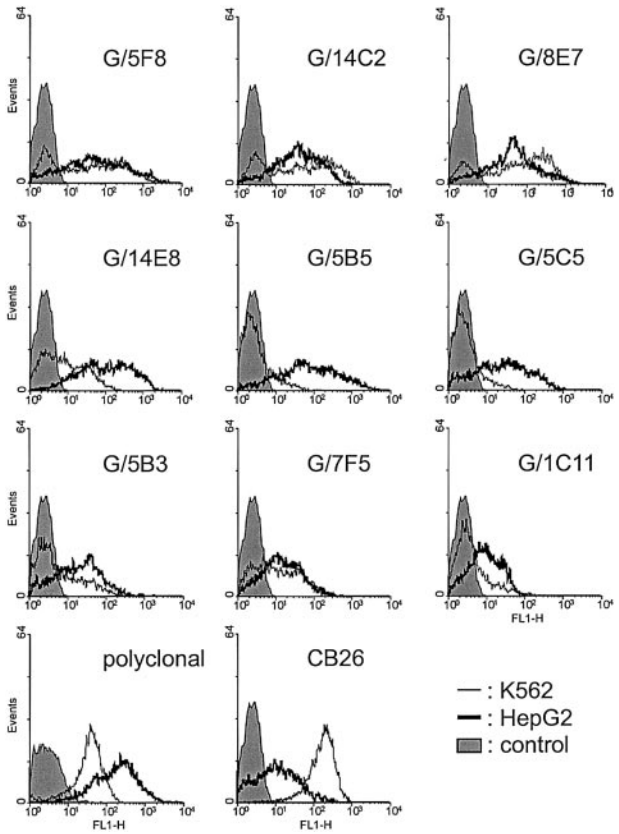

Figure 2. Reactivity of the mAbs and polyclonal antiserum against K562 and HepG2 cell lines. The 9 mAbs and the polyclonal antiserum were reacted in IIF with K562 (thin line) and HepG2 (thick line) cells. Gray profiles show the staining obtained by using an irrelevant antibody. The anti–TFR-1 CB26 mAb was used as a comparison. X-axis, fluorescence intensity/cells; y-axis, number of cells registered/channel.

sera of more than 20 mice. Polyclonal serum (8 mL) was rendered specific by absorption (vol/vol) with mock-transfected NIH-3T3 cells. The resultant polyclonal antiserum was tested in IIF against NIH-3T3/TFR-2/4B1 transfectants and representative cell lines. Results indicated that the reactivity of the polyclonal antiserum overlapped with that observed using the mAbs in the different target cells examined (Figures 1-2).

Specificity of the mAbs and the polyclonal antiserum produced

Specificity of the mAbs and antiserum selected was confirmed by reacting with mouse fibroblasts transfected with the human TFR-1. The absence of binding ruled out any cross-reactivity with human TFR-1. Similar experiments were performed on the HL-60 cell line (constitutively TFR-1$^+$), and the same reactivity pattern was obtained (Figure 3A).

Western blot analysis of the target structure

Western blot analysis was used to identify the structure recognized by the mAbs and the polyclonal antiserum and to confirm the specificity of the reaction. G/14E8 mAb, recognized as a major band of −90 kDa in HepG2, K562, and NIH-3T3/TFR-2/4B1 cells (Figure 3B). The same band was absent in mock-transfected NIH-3T3 cells. No reactivity was detectable with lysates from HL-60 cells (TFR-2$^-$ and TFR-1$^+$) or from murine L-fibroblasts transfected with human TFR-1 (L-CD71$^+$). A minor band of −105 kDa was observed in K562 cells (arrow). Similar results were obtained using mAbs G/14C2 and G/1C11 (not shown). Polyclonal antiserum confirmed the reactivity pattern (not shown).

These results were in full agreement with the RT-PCR results, which showed that the TFR-2 transcript is present only in HepG2, K562, and NIH-3T3/TFR-2/4B1 cells (Figure 3C).

Distribution of the human TFR-2 molecule in continuous cell lines and normal cells

The TFR-2 molecule is widely expressed by cell lines derived from solid tumors of different origins, including stomach, colon, liver, pancreas, breast, prostate, and brain, although with different epitope densities. Only selected B and myeloid cell lines expressed TFR-2 in the hematologic compartment. No IIF reactivity was found in T or natural killer (NK) line models. Table 1 summarizes the results obtained, expressed as mean fluorescence intensity (MFI) of mAbs representative of the A and B groups, respectively.

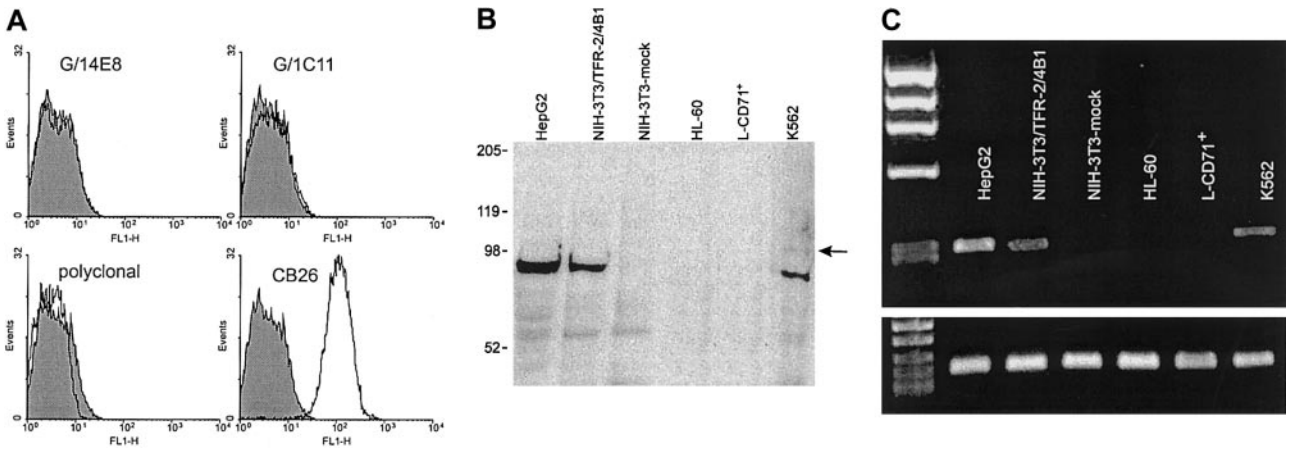

Figure 3. Analysis of the specificity of the selected mAbs and their molecular targets. (A) IIF analysis performed on L-CD71$^+$ fibroblasts reveals that the mAbs do not cross-react with TFR-1. Selected mAbs are representative for groups A (G/14E8) and B (G/1C11). The polyclonal antiserum features the same reactivity pattern. The same cells are clearly stained by the anti–TFR-1 mAb CB26. Gray profiles show the staining obtained by using an irrelevant antibody. X-axis, fluorescence intensity/cells; y-axis, number of cells registered/channel. (B) Transfectants and cell lines were lysed, run in 6% SDS-PAGE under reducing conditions, and transferred to a nitrocellulose membrane. G/14E8 mAb reacted with a dominant band of approximately 90 kDa in HepG2, in NIH-3T3/TFR-2/4B1, and in K562. A minor band of −105 kDa was observed in K562 cells (arrow). Lysates from NIH-3T3 mock-transfected cells and from HL-60 and L-CD71$^+$ fibroblasts did not show any detectable bands. The reaction was revealed using a CDP-STAR chemiluminescence reagent, and the membranes were subjected to autoradiography. (C) RT-PCR analysis of a TFR-2 fragment confirmed the presence of the relevant message in HepG2, in NIH-3T3/TFR-2/4B1, and in K562 cells. Mock-transfected NIH-3T3 cells, HL-60 cells, and L-CD71$^+$ fibroblasts did not show any message for TFR-2. GAPDH is shown as a control of RNA quality.

Distribution of the human TFR-2 in normal tissues

Tissue distribution of TFR-2 was initially evaluated by assaying the reactivity of the panel of mAbs with frozen or formalin-fixed sections from nonpathologic liver, selected as reported to display high levels of TFR-2 mRNA. Reactivity of the anti–TFR-2 mAbs was comparatively evaluated with the expression of TFR-1, as recognized by specific mAbs. TFR-2 and TFR-1 proteins were localized in serial tissue sections by using an immunoperoxidase method. Results indicated that 3 of 9 mAbs—G/5F8, G/14C2, and G/1C11—displayed clear reactivity with the frozen samples, which was maintained when the tissue was formalin fixed (Figure 4A-C). These mAbs were used for a detailed analysis of TFR-2 distribution in normal liver. The results indicate (1) that TFR-2 was present at high density in hepatocytes, (2) that reactivity was prevalently cytosolic (Figure 5D-E), and (3) that quantitative or qualitative differences were not apparent among the specimens analyzed (3 normal livers). TFR-2 was undetectable in epithelial cells of the bile ducts or in endothelial cells lining the vessels (Figure 4D, arrows). Reactivity was specific, as inferred from the use of isotype-matched mAb controls (not shown). TFR-1 protein displayed an almost overlapping expression and localization (Figure 4F-G).

The next target was the gastrointestinal (GI) tract, focusing on the duodenal tract. At low magnification, TFR-2 was widely distributed along the crypt/villus axis, with some crypts intensely stained and homogeneous expression in the villi (Figure 5A). TFR-2 molecules were evenly distributed within the cytoplasm, with a more intense signal localized on the basolateral membrane of crypt cells, whereas it was absent on nuclei (Figure 5B). TFR-2 expression by crypt cells was predominant in the duodenal specimen: in lower portions of the small intestine, the molecule was still present on villi, although with lesser intensity, but it was nearly completely lost in the crypts. Epithelial cells in the esophagus, stomach, colon, and rectum are constantly TFR-2$^-$. TFR-1 proteins were expressed by the epithelial cells of the crypts and the villi, with an intensity that decreased while epithelial cells migrated apically toward the villus tip (Figure 5D-E).

TFR-2 expression was seen among a subpopulation of lamina propria lymphocytes, in which TFR-1 is also present at high density (Figure 5B,E, arrows). Samples from normal adult pancreas, lungs, ovaries, uterus, breast, prostate, and adrenals were not stained by the TFR-2 mAbs.

Functional behavior in response to TF

In vivo functions of TFR-2 remain elusive in spite of an important sequence similarity with canonical TFR-1. Previous reports have shown that it may mediate iron uptake, displaying an affinity for TF reduced approximately 25-fold, hinting that this may not be the principal or single function of TFR-2.[22]

Exposure of K562 to HOLO-TF induces TFR-2 up-regulation at all the concentrations used. The event starts after 60 to 90 minutes of incubation and peaks approximately 4 hours later (Figure 6).

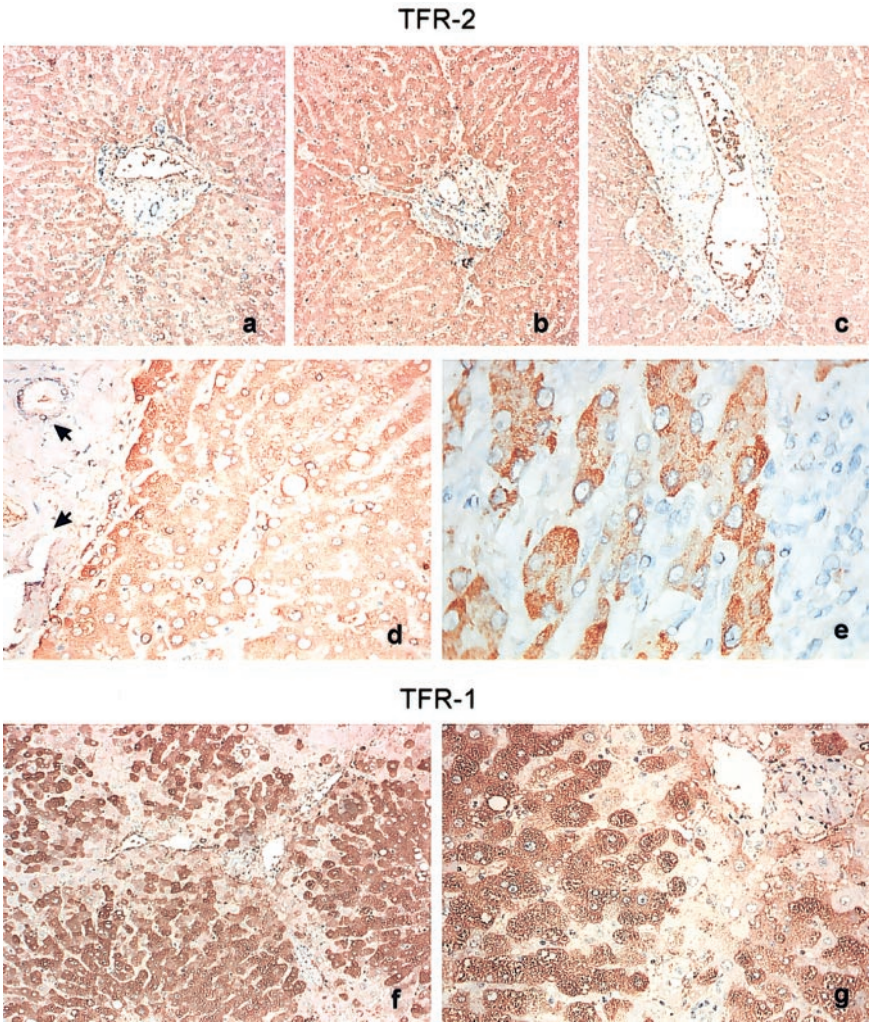

Figure 4. Immunohistochemistry analysis of TFR-2 and TFR-1 molecules in human liver. Three of 9 mAbs (A, G/5F8; B, G/14C2; C, G/1C11) clearly react with TFR-2 in normal formalin-fixed and paraffin-embedded liver tissue sections (original magnification, panels A-C, × 10). The reactivity is confined to hepatocytes and is strongly cytoplasmic (original magnification, panel E, × 100), whereas endothelial or bile duct cells are not stained (D, arrows; original magnification, × 40). (D,E) Images taken by using the G/5F8 mAb. TFR-1 protein displays an almost overlapping expression and localization (original magnifications, panel F, × 10; panel G, × 40). Representative data from 3 separate specimens are shown.

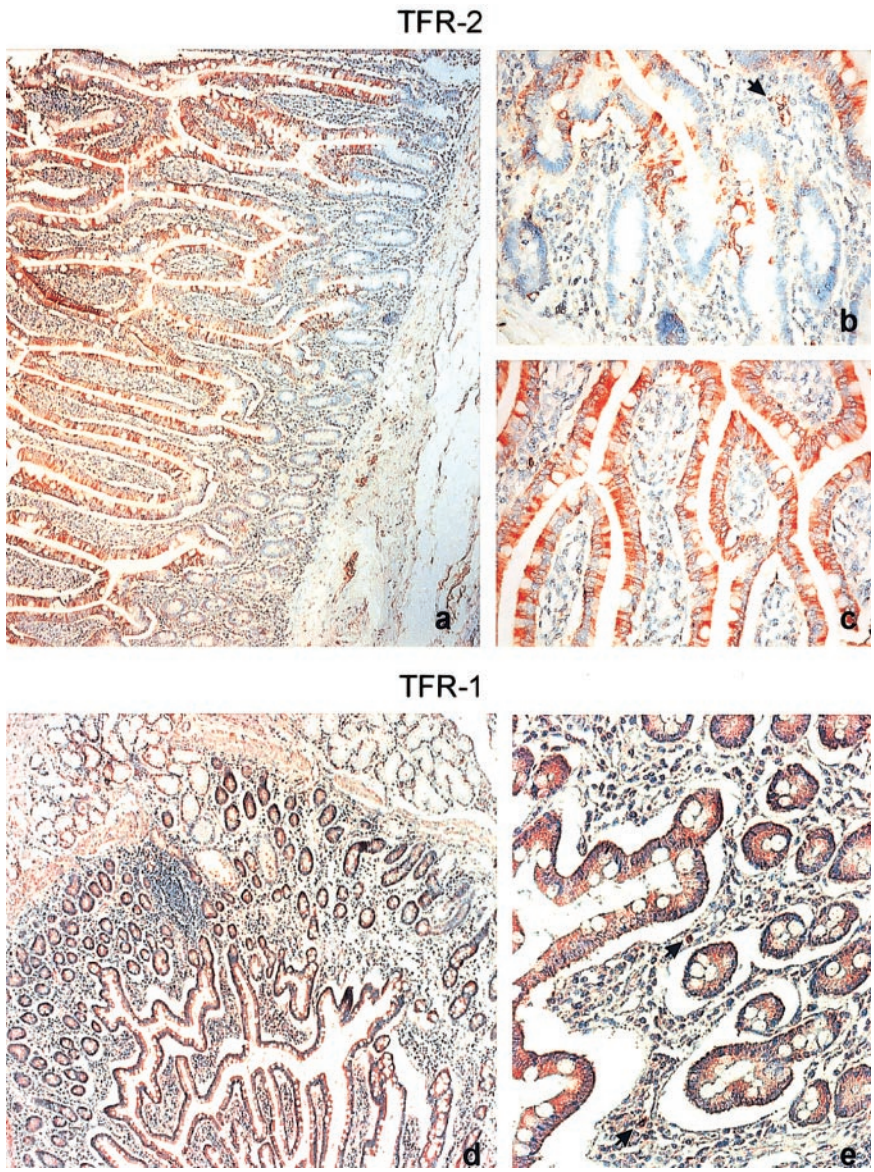

Figure 5. Immunohistochemistry analysis of TFR-2 and TFR-1 molecules in small intestine. Immunoperoxidase staining of the TFR-2 protein shows that the signal is widely distributed along the crypt/villus axis (A; original magnification, × 10), with some cells intensely stained in the crypts (B; original magnification, × 40), whereas the villus is homogeneously stained (C; original magnification, × 40). The reactivity is mostly cytoplasmic, without nuclear staining (B,C). Some lamina propria leukocytes are stained (B,E, arrows). TFR-1 protein is detectable in the crypts and villi, with diffuse intracellular and basolateral membrane-associated localizations (D, original magnification, × 10; and E, original magnification, × 40). Representative pictures from 3 different specimens are shown. TFR-2 protein was stained using G/14C2 mAb.

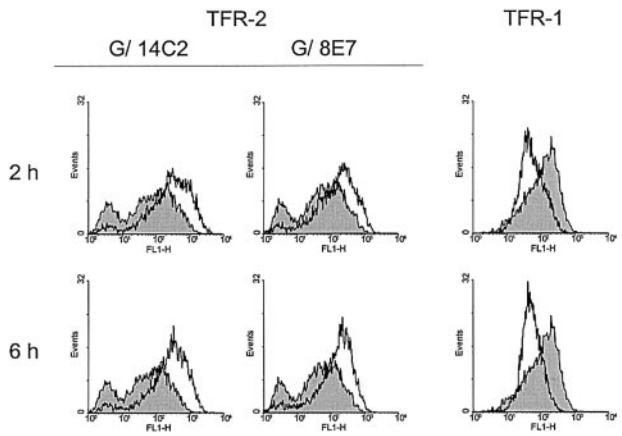

Figure 6. Modulation of TFR-2 expression by TF in K562 cells. K562 cells were exposed to HOLO-TF and tested for surface expression of TFR-2 after 2 and 6 hours, respectively (white profiles), using 2 different specific mAbs, namely G/14E8 and G/8E7. Gray profiles show the expression of TFR-2 in basal culture conditions. TFR-1 expression was used as control, with the same indications. Representative data from 4 independent experiments are shown.

TFR-2 proteins appear to cluster in selected areas of the membrane, conferring on the cell surface a spotlike appearance. The expression of the molecule was unmodified by the addition of APO-TF, independent of the concentration used. This response to HOLO-TF is reciprocal to the one described for TFR-1, which is readily (30-60 minutes) internalized under the same experimental conditions (Figure 6). Similar experiments were performed using the HepG2 cell line, grown on coverslips. Results indicated that the molecule was localized in selected areas of the membrane (Figure 7, top left panel) and that the expression was increased after 2 hours, especially in cell-cell contacts (middle left panel). Morphologic changes in the cells became evident after 6 hours, resulting in a stretched silhouette with long cytoplasmic buds. The expression of TFR-2 by these cells was highly increased and redistributed to the entire surface of the cell, accumulating in areas of contact and in the cytoplasmic filaments (bottom panel). No changes in expression could be highlighted when incubating the HepG2 cells with APO-TF. The addition of HOLO-TF to U251 brought marked up-regulation of the TFR-2 protein, similar in kinetics to the effects observed in HepG2 (Figure 7, right side). Exposure to APO-TF did not yield detectable effects on the surface expression of TFR-2.

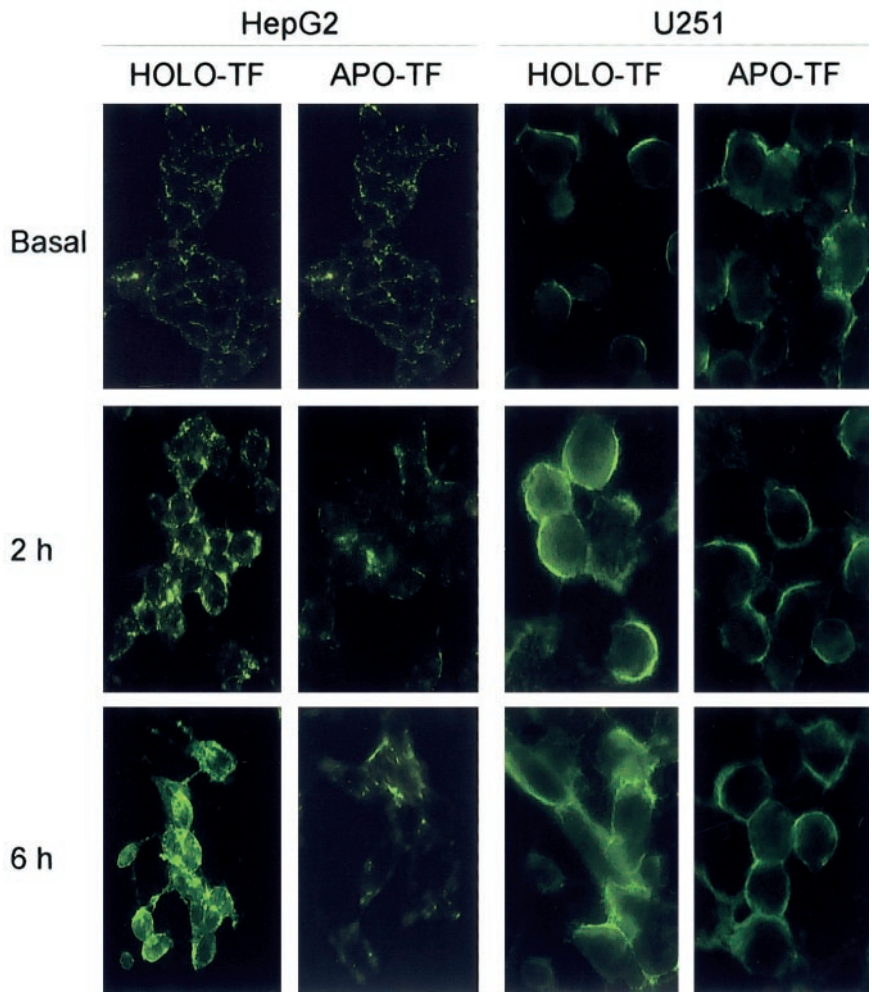

Figure 7. TF influence on TFR-2 expression in adherent cells. HepG2 (hepatocarcinoma) and U251 (glioblastoma) were grown on coverslips, exposed to TF for 2 and 6 hours, respectively, and evaluated for TFR-2 expression. Results show the presence of discrete membrane areas in which TFR-2 is localized, more apparent in basal and in 2-hour conditions. In vitro incubation is paralleled by a constant increase in TFR-2 expression, which appears uniformly deployed on the surface after 6-hour incubation. The observed effects are dependent on the presence of HOLO-TF. APO-TF was ineffective in inducing detectable or comparable effects. TFR-2 protein was stained using G/14C2 mAb. Representative images from 5 independent experiments are shown.

Discussion

The biologic functions and tissue distribution of TFR-2 remain undefined. Experimental evidence indicates that TFR-2 may mediate iron uptake; however, its affinity for iron-loaded TF is remarkably lower than that of TFR-1,[6,22] suggesting that iron uptake is not the principal or the only function of TFR-2. Inactivation of TFR-2 causes a form of HH with features similar to those of *HFE*-related HH,[8-10] hinting at a regulatory role for TFR-2 in iron metabolism. Most available data concern TFR-2 mRNA expression, whereas studies on the protein were limited by the lack of specific reagents. To investigate its structure, tissue distribution, and function(s), we developed 9 murine mAbs and a murine polyclonal antiserum against TFR-2, exploiting a highly sensitive immunization protocol and adopting screening strategies derived from the experience of the CD Workshop on Differentiation Antigens (Harrowgate, United Kingdom, June 16-22, 2000).

Results provide a preliminary structural blueprint of human TFR-2 based on the identification of discrete domains of the molecule, an analysis of TFR-2 tissue distribution, and information about receptor behavior following exposure to the TF ligand. The finding that only 3 of 9 selected mAbs clearly reacted with the liver sections indicates the existence of 2 major epitopes of the TFR-2 molecule, as seen from for the murine immune system. These epitopes are under analysis by walking on the molecule using peptides spanning the TFR-2 sequence and by testing the signaling potential of the specific mAbs and the polyclonal antiserum.

Western blot analyses confirm that the mAbs are specific for TFR-2, reacting with a dominant band of −90 kDa in HepG2 along with a minor band of −105 kDa in K562 cell lines. Other minor components are stained by the different mAbs and confirmed by the antiserum. The presence of tissue-specific isoforms or of cell-specific glycosylation is a matter for further investigation.

The analysis of TFR-2 distribution in different tissues indicates that the protein is prevalently expressed by cells that play a prominent role in the regulation of iron homeostasis. Indeed, high levels of expression were found in hepatocytes, a major iron-storage site, and in the enterocytes of the crypts and villi, localized in the portions of the GI tract involved in iron absorption. The distribution of TFR-2 was strikingly different from that of TFR-1 in normal tissues not taking part in the regulation of iron metabolism and in continuous cell lines (data not shown), but it was similar in liver and small intestine, suggesting a role of TFR-2 in the regulation of iron homeostasis. According to a current hypothesis, the sensing of body iron needs is carried out by the crypt cells and likely involves the uptake of iron from circulating TF.[23-25] In agreement with this view, impaired iron uptake from plasma TF has been reported in a murine model of HFE-related HH.[26] TFR-1 represents a component of the body iron sensor by directly interacting with HFE in the epithelial cells of the crypts.[27] It is still unproved whether TFR-2, expressed by the basolateral membrane of duodenal crypt cells as TFR-1, interacts with HFE to play a role in iron sensing.[25] Direct binding between HFE and TFR-2 has been ruled out by using soluble forms of these proteins,[22] although in vivo interactions or colocalization have not been conclusively

established. As a receptor able to bind TF on the basolateral membrane of the crypt cells, TFR-2 might represent a second sensor of body iron or might participate in a more complex sensing mechanism, as recently hypothesized.[28] The effect of inactivation of TFR-2 by mutations in HH type 3 is in keeping with the loss of a component of the sensing machinery.

The expression of TFR-2 in gut differs from that of DMT1/nramp2, the luminal iron transporter, which localizes prevalently in the enterocytes of the villi and is strongly induced in conditions of iron deficiency in the villus brush border.[29,30] The distribution of TFR-2 parallels that of TFR-1, also in liver tissue, while it differs from that of HFE. TFR-2 is expressed exclusively by hepatocytes, whereas it is undetectable in bile duct cells and in the cells lining the sinusoids, all reported as HFE^{+}.[31]

The finding that TFR-2 appears to be predominantly cytoplasmic in liver sections is surprising, at least in view of its reported similarity with TFR-1. It is possible that this is simply because of technical limits in observing the molecule in histologic sections. Alternatively, it might reflect the physiologic conditions of the liver tissues examined. This does not preclude that TFR-2 may gain access to the hepatocyte membrane in other metabolic or abnormal conditions on external or internal signals.

We investigated the physiologic role of TFR-2 by analyzing the effects elicited by exposing cells in suspension and in adherence to HOLO-TF. HOLO-TF clearly up-regulates TFR-2, inducing clustering of the molecule in different membrane areas, while down-regulating TFR-1. No effects were observed in response to APO-TF. Exposure of the cells to inorganic iron or to iron deprivation induced by desferrioxamine did not quantitatively change TFR-2 expression levels nor its localization (data not shown), in line with the reported iron independence of TFR-2.[11] These results, confirmed in cell lines of different origin, suggest that TFR-2 access and clustering to the membrane may provide some sort of flag related to the TFR-1 endocytic pathway. This behavior is compatible with the hypothesized function of TFR-2 as an iron sensor and suggests that the regulatory function of the molecule is linked to that of TFR1.

In conclusion, we consider the label TFR-2 to be a possible misnomer; transferrin-binding activity may be only one aspect of the functions of the molecule. Multitask molecules are proving not to be the exception but the rule. To cite one related instance, the TFR-1 molecule transports TF and also operates as a receptor for IgA in the kidney.[32] Supporting evidence for the pleiotropic view of the molecule may come from the description of the role of TFR-2 in iron metabolism and in the cross-talk among cells regulating iron uptake. Of key relevance will be the use of the reagents developed for the present work to study disease models and the signals mediated by TFR-2 engagement.

References

1. Ponka P, Lok CN. The transferrin receptor: role in health and disease. Int J Biochem Cell Biol. 1999; 31:1111-1137.
2. Richardson DR, Ponka P. The molecular mechanisms of the metabolism and transport of iron in normal and neoplastic cells. Biochim Biophys Acta. 1997;1331:1-40.
3. Trinder D, Zak O, Aisen P. Transferrin receptor-independent uptake of differic transferrin by human hepatoma cells with antisense inhibition of receptor expression. Hepatology. 1996;23:1512-1520.
4. Kawabata H, Yang R, Hirama T, et al. Molecular cloning of transferrin receptor 2: a new member of the transferrin receptor-like family. J Biol Chem. 1999;274:20826-20832.
5. Kawabata H, Nakamaki T, Ikonomi P, Smith RD, Germain RS, Koeffler HP. Expression of transferrin receptor 2 in normal and neoplastic hematopoietic cells. Blood. 2001;98:2714-2719.
6. Kawabata H, Germain RS, Vuong PT, Nakamaki T, Said JW, Koeffler HP. Transferrin receptor 2-alpha supports cell growth both in iron-chelated cultured cells and in vivo. J Biol Chem. 2000;275: 16618-16625.
7. Levy JE, Jin O, Fujiwara Y, Kuo F, Andrews NC. Transferrin receptor is necessary for development of erythrocytes and the nervous system. Nat Genet. 1999;21:396-399.
8. Camaschella C, Roetto A, Cali A, et al. The gene TFR2 is mutated in a new type of hemochromatosis mapping to 7q22. Nat Genet. 2000;25:14-15.
9. Roetto A, Totaro A, Piperno A, et al. New mutations inactivating transferrin receptor 2 in hemochromatosis type 3. Blood. 2001;97:2555-2560.
10. Girelli D, Bozzini C, Roetto A, et al. Clinical and histopathological findings in a family with hemochromatosis type 3, carrying a new mutation in transferrin receptor 2 gene. Gastroenterology. 2002;122:1295-1302.
11. Fleming RE, Migas MC, Holden CC, et al. Transferrin receptor 2: continued expression in mouse liver in the face of iron overload and in hereditary hemochromatosis. Proc Natl Acad Sci U S A. 2000;97:2214-2219.
12. Kawabata H, Germain RS, Ikezoe T, et al. Regulation of expression of murine transferrin receptor 2. Blood. 2001;98:1949-1954.
13. Deaglio S, Zubiaur M, Gregorini A, et al. Human CD38 and CD16 are functionally dependent and physically associated in natural killer cells. Blood. 2002;99:2490-2498.
14. Peruzzi L, Melioli G, De Monte LB, et al. Microplate selection technique (MPST): a new method for selecting mouse transfectants expressing human gene products. J Immunol Methods. 1989; 123:113-121.
15. Funaro A, Spagnoli GC, Ausiello CM, et al. Involvement of the multilineage CD38 molecule in a unique pathway of cell activation and proliferation. J Immunol. 1990;145:2390-2396.
16. Deaglio S, Dianzani U, Horenstein AL, et al. Human CD38 ligand: a 120-kDa protein predominantly expressed on endothelial cells. J Immunol. 1996;156:727-734.
17. Deaglio S, Morra M, Mallone R, et al. Human CD38 (ADP-ribosyl cyclase) is a counter-receptor of CD31, an Ig superfamily member. J Immunol. 1998;160:395-402.
18. DeMonte LB, Nistico P, Tecce R, et al. Gene transfer by retrovirus-derived shuttle vectors in the generation of murine bispecific monoclonal antibodies. Proc Natl Acad Sci U S A. 1990;87: 2941-2945.
19. Zubiaur M, Fernandez O, Ferrero E, et al. CD38 is associated with lipid rafts and upon receptor stimulation leads to Akt/protein kinase B and Erk activation in the absence of the CD3-ζ immune receptor tyrosine-based activation motifs. J Biol Chem. 2002;277:13-22.
20. Sapino A, Bongiovanni M, Cassoni P, et al. Expression of CD31 by cells of extensive ductal in situ and invasive carcinomas of the breast. J Pathol. 2001;194:254-261.
21. Fernandez JE, Deaglio S, Donati D, et al. Analysis of the distribution of human CD38 and of its ligand CD31 in normal tissues. J Biol Regul Homeost Agents. 1998;12:81-91.
22. West AP Jr, Bennett MJ, Sellers VM, Andrews NC, Enns CA, Bjorkman PJ. Comparison of the interactions of transferrin receptor and transferrin receptor 2 with transferrin and the hereditary hemochromatosis protein HFE. J Biol Chem. 2000;275:38135-38138.
23. Taylor MR, Gatenby PB. Iron absorption in relation to transferrin saturation and other factors. Br J Haematol. 1966;12:747-753.
24. Andrews NC. Iron metabolism: iron deficiency and iron overload. Annu Rev Genomics Hum Genet. 2000;1:75-98
25. Roy CN, Enns CA. Iron homeostasis: new tales from the crypt. Blood. 2000;96:4020-4027.
26. Trinder D, Olynyk JK, Sly WS, Morgan EH. Iron uptake from plasma transferrin by the duodenum is impaired in the Hfe knockout mouse. Proc Natl Acad Sci U S A. 2002;99:5622-5626.
27. Waheed A, Parkkila S, Saarnio J, et al. Association of HFE protein with transferrin receptor in crypt enterocytes of human duodenum. Proc Natl Acad Sci U S A. 1999;96:1579-1584.
28. Townsend A, Drakesmith H. Role of HFE in iron metabolism, hereditary haemochromatosis, anaemia of chronic disease, and secondary iron overload. Lancet. 2002;359:786-790.
29. Trinder D, Oates PS, Thomas C, Sadleir J, Morgan EH. Localisation of divalent metal transporter 1 (DMT1) to the microvillus membrane of rat duodenal enterocytes in iron deficiency, but to hepatocytes in iron overload. Gut. 2000;46:270-276.
30. Canonne-Hergaux F, Levy JE, Fleming MD, Montross LK, Andrews NC, Gros P. Expression of the DMT1 (NRAMP2/DCT1) iron transporter in mice with genetic iron overload disorders. Blood. 2001; 97:1138-1140.
31. Parkkila S, Waheed A, Britton RS, et al. Immunohistochemistry of HLA-H, the protein defective in patients with hereditary hemochromatosis, reveals unique pattern of expression in gastrointestinal tract. Proc Natl Acad Sci U S A. 1997;94: 2534-2539.
32. Moura IC, Centelles MN, Arcos-Fajardo M, et al. Identification of the transferrin receptor as a novel immunoglobulin (Ig)A1 receptor and its enhanced expression on mesangial cells in IgA nephropathy. J Exp Med. 2001;194:417-425.